Stimuli-Responsive Spin Crossover Behavior in 3D Fe(II) Porous Coordination Polymer for Guest Molecules

Li Sun[a], Xiaochun Li[a], Constance Vandenbulcke[a], Nour El Islam Belmouri[b], Guillaume Bouchez[b], Koen Robeyns[a], Aurelian Rotaru[c], Kamel Boukheddaden[b] and Yann Garcia[a]*

[a]Institute of Condensed Matter and Nanosciences, Molecular Chemistry, Materials and Catalysis (IMCN/MOST), Université catholique de Louvain, 1348 Louvain-la-Neuve, Belgium.

[b]Université Paris-Saclay, UVSQ, CNRS, GEMAC UMR 8635, 45 Avenue des Etats Unis, F78035 Versailles Cedex, France

[c]Department of Electrical Engineering and Computer Science and MANSiD Research Center, "Stefan cel Mare" University, University Street, 13, Suceava 720229, Romania

Contents:

Characterization methods

Elemental analyses for C, H, and N were performed by Medac Ltd (UK). Fourier-transformed infrared (FT-IR) spectroscopy measurements were performed using an Equinox 55 (Bruker) equipped with an ATR modulus and an MCT detector. The Bruker software OPUS was used for data treatment (including ATR correction). DSC measurements were performed on a Mettler Toledo DSC with an $N_{2(g)}$ atmosphere at a heating rate of 2 K/min from 113 K to 298 K. Powder X-ray diffraction (PXRD) patterns were collected on a D8-Advance diffractometer (Bruker, Germany) with Cu Kα radiation (λ = 1.5148 Å) operating at 40 kV and 30 mA. Magnetic susceptibilities were measured on a Quantum design MPMS-5s SQUID magnetometer. Magnetic data were corrected for the sample holder and diamagnetic contributions. The crystal sample was quickly loaded into a gelatin capsule and immediately inserted within the SQUID cavity.

Crystallographic data collection and structure determination

Suitable crystals were selected for single-crystal X-ray diffraction analysis. X-ray intensity data for **1** and **3** were collected at 100 K and 298 K on a MAR345 image plate using MoKα radiation (λ = 0.71073Å). Data were integrated by CrysalisAlisPro (Agilent Technologies UK Ltd., Oxford, U.K., Xcalibur/Super Nova CCD system, CrysAlisPro Software system, versions 1.171.37.35) Absorption correction was applied using the integrated multiscan absorption algorithm. The structures were determined by direct methods (SHELXS) and refined by full-matrix least squares on F^2 using SHELXL2014.[1] (The location of the Fe atom was easily determined, and N and C atoms were subsequently located in the Fourier difference maps. The non-hydrogen atoms were refined anisotropically. The H atoms were introduced in calculated positions and refined with fixed geometry with respect to their carrier atoms. Disordered $CHCl_3$ and CH_3OH molecules could not be modelled properly. Thus, we have used the program SQUEEZE, a part of the PLATON package of crystallographic software, to calculate the solvent disorder area and move away their contributions to the overall intensity data.

Summary of shortest inter contacts with d(I-J) < R(I) + R(J) + 0.2

Nr	d(min)	Del	X	- At(I)		At(J)	-Y	descriptor
1	3.1400	-0.16	C42	- N43	...	Cl76	-C75	<
2	2.5600	-0.74	C45	- N46	...	*Cl8 B	-C81B	<<
3	2.9700	-0.33	C45	- N46	...	*Cl8 D	-C81C	<<
4	3.3500	-0.10	C8	- C9	...	Cl77	-C75	<
5	2.9200	-0.03	C7	- H7	...	*Cl83	-C81	<
6	2.5600	-0.16	C34	- H34	...	O57	-Cl55	<
7	2.5800	-0.14	C38	- H38	...	O57	-Cl55	<
8	3.1400	-0.16	C42	- N43	...	Cl76	-C75	<
9	2.5600	-0.74	C45	- N46	...	*Cl8 B	-C81B	<<
10	2.9700	-0.33	C45	- N46	...	*Cl8 D	-C81C	<<
11	3.3500	-0.10	C8	- C9	...	Cl77	-C75	<
12	2.9200	-0.03	C7	- H7	...	*Cl83	-C81	<
13	2.5600	-0.16	C34	- H34	...	O57	-Cl55	<
14	2.5800	-0.14	38	- H38	...	O57	-Cl55	<
15	3.1400	-0.16	C42	- N43	...	Cl76	-C75	<
16	2.5600	-0.74	C45	- N46	...	*Cl8 B	-C81B	<<
17	2.9700	-0.33	C45	- N46	...	*Cl8 D	-C81C	<<
18	3.3500	-0.10	C8	- C9	...	Cl77	-C75	<
19	2.9200	-0.03	C7	- H7	...	*Cl83	-C81	<
20	2.5600	-0.16	C34	- H34	...	O57	-Cl55	<
21	2.5800	-0.14	C38	- H38	...	O57	-Cl55	<
22	3.1400	-0.16	C42	- N43	...	Cl76	-C75	<
23	2.5600	-0.16	C34	- H34	...	O57	-Cl55	<
24	2.5600	-0.74	C45	- N46	...	*Cl8 B	-C81B	<<
25	2.9700	-0.33	C45	- N46	...	*Cl8 D	-C81C	<<
26	3.0700	-0.38	C5	- C6	...	*Cl70	-C69	<<
27	2.5600	-0.74	C45	- N46	...	*Cl8 B	-C81B	<<
28	2.9700	-0.33	C45	- N46	...	*Cl8 D	-C81C	<<
29	3.3500	-0.10	C8	- C9	...	Cl77	-C75	<
30	2.9200	-0.03	C7	- H7	...	*Cl83	-C81	<
31	2.5800	-0.14	C38	- H38	...	O57	-Cl55	<
32	3.1400	-0.16	C42	- N43	...	Cl76	-C75	<
33	2.5600	-0.74	C45	- N46	...	*Cl8 B	-C81B	<<
34	2.9700	-0.33	C45	- N46	...	*Cl8 D	-C81C	<<
35	3.0700	-0.38	C5	- C6	...	*Cl70	-C69	<<
36	2.5600	-0.74	C45	- N46	...	*Cl8 B	-C81B	<<
37	2.9700	-0.33	C45	- N46	...	*Cl8 D	-C81C	<<
38	3.3500	-0.10	C8	- C9	...	Cl77	-C75	<
39	2.9200	-0.03	C7	- H7	...	*Cl83	-C81	<

40	2.5800	-0.14	C38	- H38	...	O57	-Cl55	<
41	3.1400	-0.16	C42	- N43	...	Cl76	-C75	<
42	2.5600	-0.74	C45	- N46	...	*Cl8 B	-C81B	<<
43	2.9700	-0.33	C45	- N46	...	*Cl8 D	-C81C	<<
44	3.0700	-0.38	C5	- C6	...	*Cl70	-C69	<<
45	2.5600	-0.74	C45	- N46	...	*Cl8 B	-C81B	<<
46	2.9700	-0.33	C45	- N46	...	*Cl8 D	-C81C	<<
47	3.3500	-0.10	C8	- C9	...	Cl77	-C75	<
48	2.9200	-0.03	C7	- H7	...	*Cl83	-C81	<
49	2.5800	-0.14	C38	- H38	...	O57	-Cl55	<
50	3.1400	-0.16	C42	- N43	...	Cl76	-C75	<
51	2.5600	-0.74	C45	- N46	...	*Cl8 B	-C81B	<<
52	2.9700	-0.33	C45	- N46	...	*Cl8 D	-C81C	<<
53	3.0700	-0.38	C5	- C6	...	*Cl70	-C69	<<
54	2.5600	-0.74	C45	- N46	...	*Cl8 B	-C81B	<<
55	2.9700	-0.33	C45	- N46	...	*Cl8 D	-C81C	<<
56	3.3500	-0.10	C8	- C9	...	Cl77	-C75	<
57	2.9200	-0.03	C7	- H7	...	*Cl83	-C81	<
58	2.5600	-0.16	C34	- H34	...	O57	-Cl55	<
59	2.5800	-0.14	C38	- H38	...	O57	-Cl55	<
60	3.1400	-0.16	C42	- N43	...	Cl76	-C75	<
61	2.5600	-0.74	C45	- N46	...	*Cl8 B	-C81B	<<
62	2.9700	-0.33	C45	- N46	...	*Cl8 D	-C81C	<<
63	3.0700	-0.38	C5	- C6	...	*Cl70	-C69	<<
64	2.5600	-0.74	C45	- N46	...	*Cl8 B	-C81B	<<
65	2.9700	-0.33	C45	- N46	...	*Cl8 D	-C81C	<<
66	2.9200	-0.03	C7	- H7	...	*Cl83	-C81	<
67	2.5600	-0.74	C45	- N46	...	*Cl8 B	-C81B	<<
68	2.9700	-0.33	C45	- N46	...	*Cl8 D	-C81C	<<
69	3.0700	-0.38	C5	- C6	...	*Cl70	-C69	<<
70	2.5600	-0.74	C45	- N46	...	*Cl8 B	-C81B	<<
71	2.9700	-0.33	C45	- N46	...	*Cl8 D	-C81C	<<
72	3.3500	-0.10	C8	- C9	...	Cl77	-C75	<
73	2.9200	-0.03	C7	- H7	...	*Cl83	-C81	<
74	2.5600	-0.16	C34	- H34	...	O57	-Cl55	<
75	2.5800	-0.14	C38	- H38	...	O57	-Cl55	<
76	3.1400	-0.16	C42	- N43	...	Cl76	-C75	<
77	2.5600	-0.74	C45	- N46	...	*Cl8 B	-C81B	<<
78	2.9700	-0.33	C45	- N46	...	*Cl8 D	-C81C	<<

79	3.0700	-0.38	C5	- C6	...	*Cl70	-C69	<<
80	2.5600	-0.74	C45	- N46	...	*Cl8B	-C81B	<<
81	2.9700	-0.33	C45	- N46	...	*Cl8D	-C81C	<<
82	2.9200	-0.03	C7	- H7	...	*Cl83	-C81	<

descriptor :: < denotes contacts less than the sum of the van der Waals Radii and << contacts less than this sum minus 0.2 Angstrom.

Optical Microscopy

Optical microscopy measurements were carried out under a primary vacuum on single crystals (length × width = 166 μm × 66 μm) using a Nikon Eclipse LV100 microscope (objective × 20, numerical aperture 0.4), equipped with a closed cycle Oxford Instruments nitrogen-flow cryostat and connected to a digital camera Coreview Dalsa Falcon 1 : 4 M100 HG color, capable of capturing up to 100 frames per second. The OM images were recorded in transmission geometry using backward illumination by a tungsten halogen lamp, provided by the microscope. The sample was mounted in specific helium-tight cell designed for optical microscopy.[2] All measurements were performed using a temperature scan rate of 1 K min^{-1}. The camera was configured to save five images per second to record the spatiotemporal behavior of the spin transition. From every saved image, we can extract the optical density (OD), defined as:

$$OD = log_{10}\left(\frac{I_{incident}}{I_{transmitted}}\right), \quad (1)$$

where $I_{incident}$ corresponds to the bright field intensity while $I_{transmitted}$ corresponds to the intensity of the transmitted light through the single crystal. The OD which is the key parameter of the OM data analysis (recorded images) directly relates to the HS fraction, n_{HS}, of molecules undergoing the spin transition in the single crystal and therefore it should not be confused with the absolute HS fraction of molecules switching between the LS and HS states in the system. Such quantity can only be obtained with an experimental technique, able to distinguish non-switching SCO molecules from switchable ones, like ^{57}Fe Mössbauer spectroscopy,[3] for example. Unfortunately, the latter is not adapted for studies on one micrometric size single crystal as OM. The HS fraction (n^*_{HS}) of metal ions in the HS state, among those switching between the two states, is then derived from OD data, through the relation[4]:

$$n^*_{HS} = \frac{< OD(x,y) > - < OD >_{LS}}{< OD >_{HS} - < OD >_{LS}}, \quad (2)$$

where $< OD >_{HS}$ and $< OD >_{LS}$ are respectively the spatially-averaged OD values in the HS and LS states and $< OD(x,y) >$ is the spatially averaged optical density over the crystal at given temperature, T. In addition, each image of the experimental OM data was split into three OD components: red, green, and blue, depending on the single crystal thickness and color. From one compound to another, the signal quality (signal to noise ratio), would perhaps be better, either in the red, green, or blue pixel. All the data are analyzed using Matlab programs developed by the Versailles group.

Modelling

The Ising model is used here to describe the SCO from the HS to the LS state by representing these states with fictitious spin states +1 and -1, respectively. The expression of the Hamiltonian of the system is given by[5]

$$H = -J\sum_{i,j} S_i S_j + \sum_i \Delta_{eff} S_i, \quad (3)$$

where, $J > 0$ or $J < 0$ represent the ferroelastic or antiferro-elastic interaction parameter between the SCO molecules. $\Delta_{eff} = (\Delta - k_B T lng)$ is the effective ligand field gap, which includes the quantity, Δ, corresponding to the difference of ligand fields between HS and LS states of isolated molecules and the entropic contribution, $k_B T lng$, resulting from the electronic and vibrational degeneracy ratio, $g = \frac{g_{HS}}{g_{LS}}$, between the HS and LS states. Using a mean-field treatment of Hamiltonian (3), which follows very standard developments, we can obtain the following homogenous free energy:

$$F_{hom} = \frac{1}{2} Jm^2 - k_B T \ln\left[2g\, cosh\left(\beta(Jm - \Delta_{eff})\right)\right], \quad (4)$$

where $m = < S >$ is the average fictitious magnetization per site and $\beta = \frac{1}{k_B T}$. The minimization of the analytical expression of the free energy, given in (4), with respect to the net "magnetization", m, resolving the equation $\frac{\partial F_{hom}}{\partial m} = 0$, leads straightforwardly to the derived self-consistent equation (5):

$$m = tanh\left[\beta(Jm - \Delta_{eff})\right], \quad (5)$$

The latter is connected to the HS fraction, n_{HS}, through the relation,

$$n_{HS} = \frac{1 + < S >}{2} = \frac{1 + m}{2}. \quad (6)$$

The resolution of the self-consistent equation (5) gives the temperature dependence of the HS fraction, n_{HS}, which represents the fraction of molecules occupying the HS state stabilized at higher temperatures. The equation (5) admits a solution, $m = 0$, when $\Delta_{eff} = \Delta - k_B T \ln g = 0$. So, for $m = 0$, corresponding to $n_{HS} = \frac{1}{2}$, we derive the transition temperature of the system which cancels the effective field, whose expression writes simply as $T_{eq} = \frac{\Delta}{k_B lng}$. It is interesting to note that the resolution of Equation (5) does not need any numerical simulations to be performed; despite the self-consistent nature of this equation, it can be easily reversed by expressing the temperature as a function of the magnetization:

$$T = \frac{2(Jm - \Delta)}{k_B \ln\left[\left(\frac{1+m}{1-m}\right)\frac{1}{g}\right]} \quad (7)$$

Then changing m from -1 to $+1$ by accounting for the limits gives, in a unique way, the associated temperature, T.

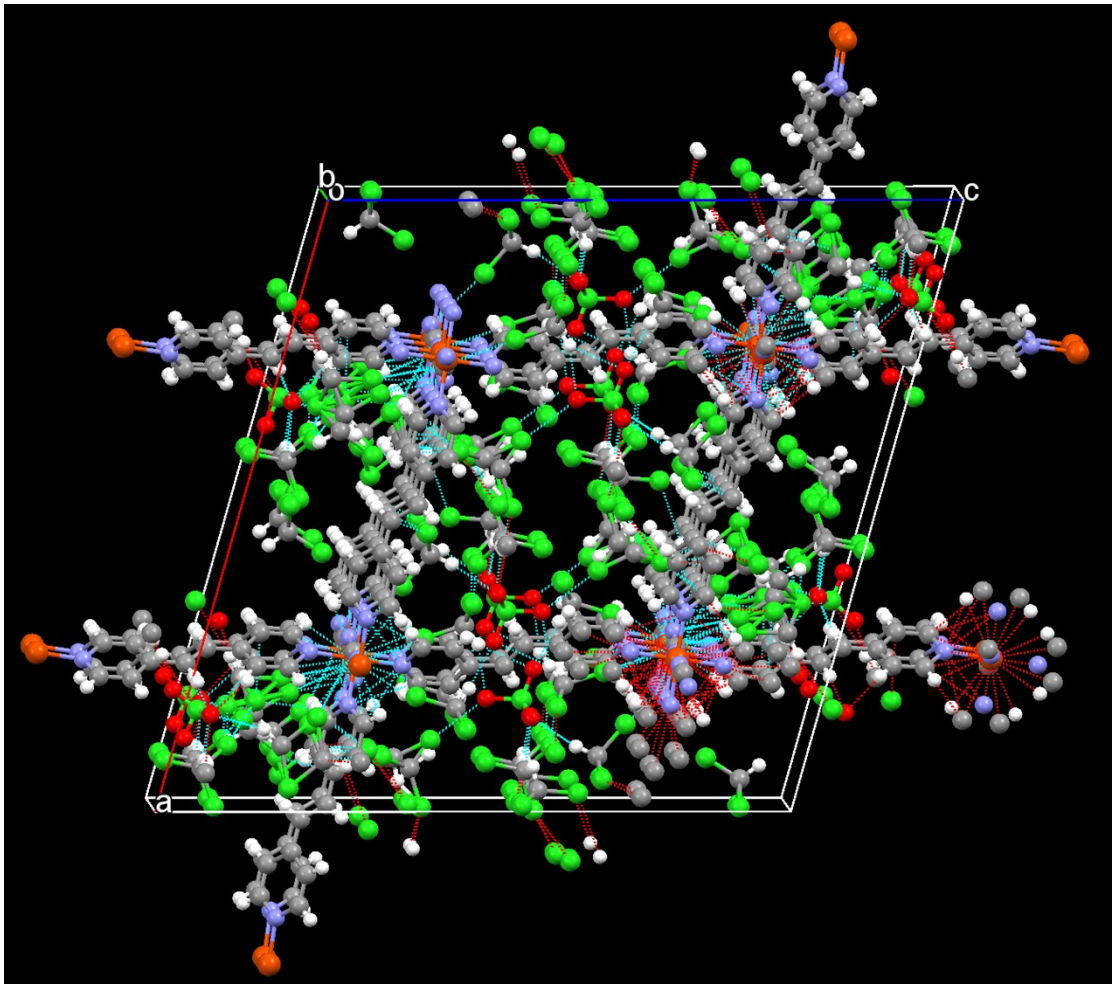

Figure **S1** Crystal structure of **1** at 100 K, viewed along the b-axis with lattice solvent molecules, Fe (orange), O (red), N (blue), C (grey), and Cl (green).

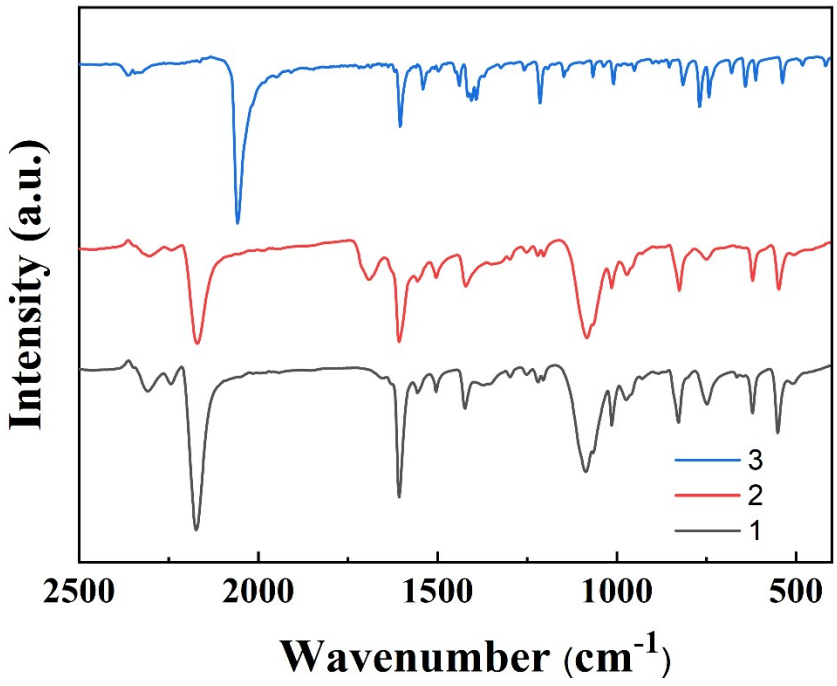

Figure **S2**. FT-IR of **1**, **2** and **3**.

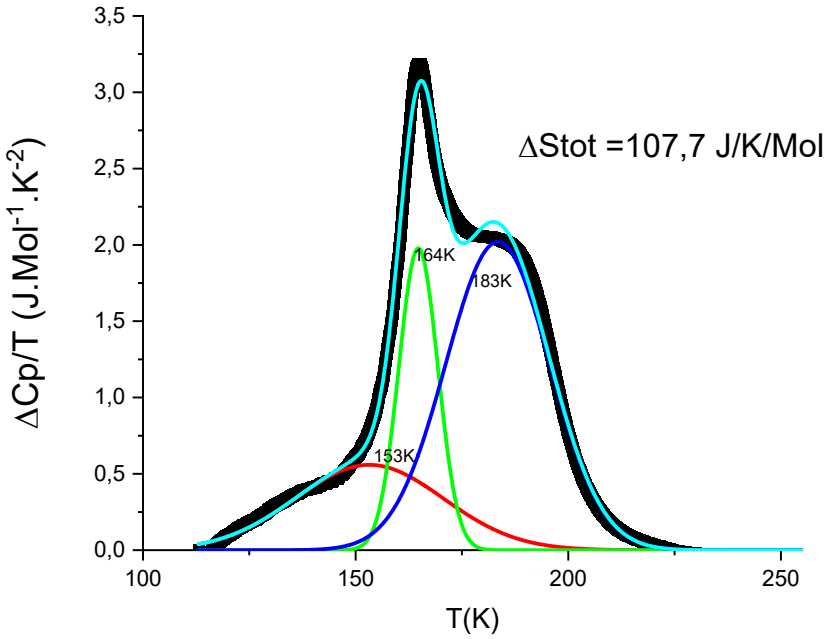

Figure **S3**. Gaussian fitting of the heat capacity excess with three contributions, derived from the experimental curve of Fig. 7a recorded on warming. The associated entropy changes are $\Delta S_1 = 24$, $\Delta S_2 = 22$, and $\Delta S_3 = 61{,}7$ J.mol^{-1}K^{-1} for the 1st , 2nd and 3rd peak respectively.

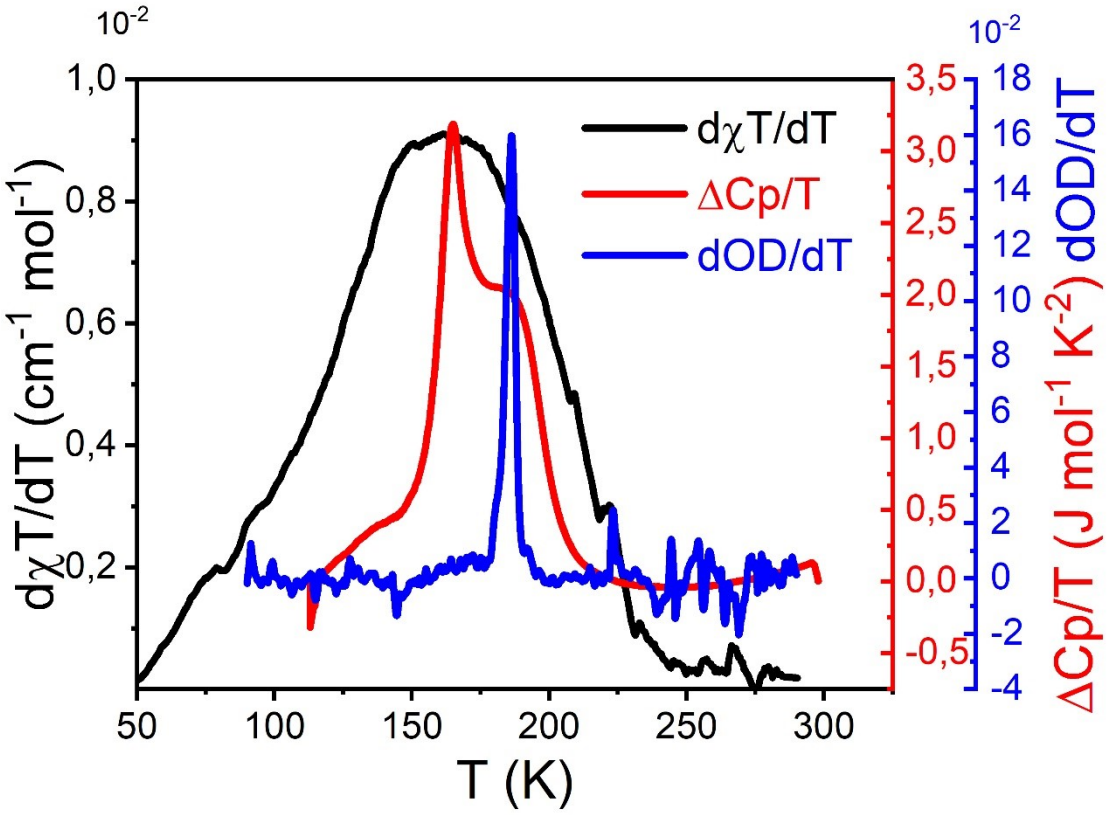

Figure **S4**. Thermal dependence of the derivative of the magnetic susceptibility (black curve) and optical density (blue curve) of **1** *vs.* temperature, compared with the heat capacity excess (red curve), related to the experimental curve of Figure 8.

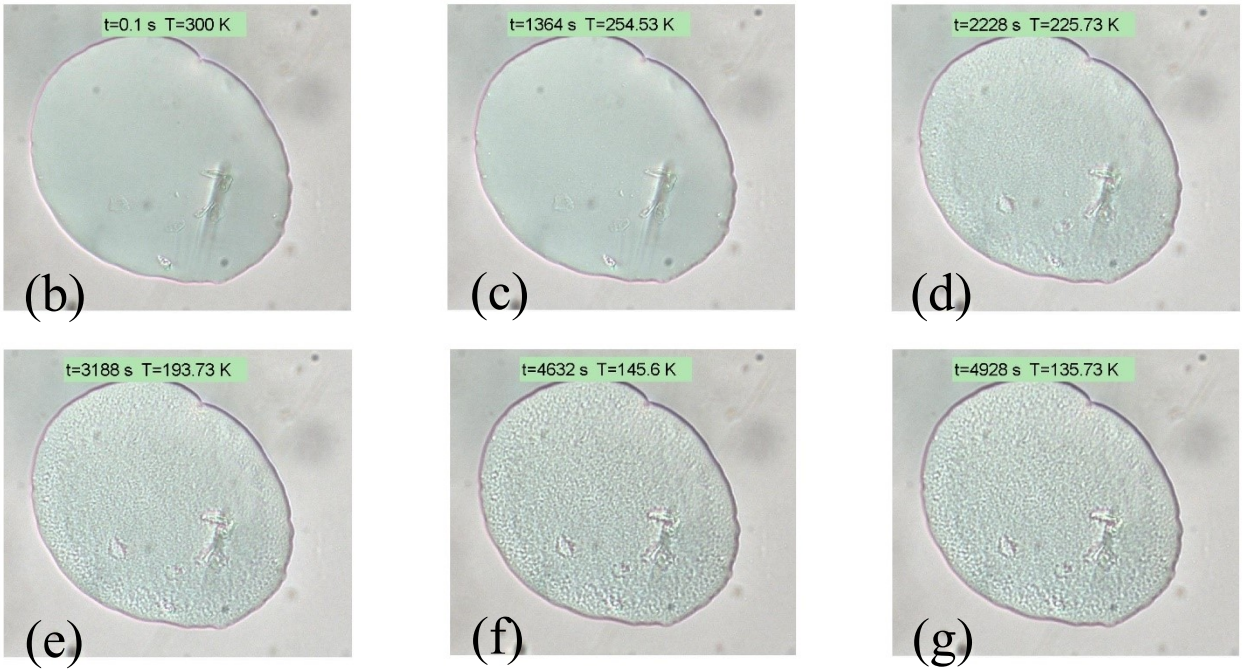

Figure **S5**. Selected snapshots of the thermal transformation of a droplet of Vaseline on cooling from 300 to ~136 K showing the occurrence of a glass transition around 200 K. The corresponding OD signal is provided in Fig. 8a in the main manuscript.

Movie 1 and Movie 2

References:

(1) Sheldrick, G.M. A short history of SHELX. *Acta Crystallogr. Sect. A: Found. Crystallogr.* **2008**, *64*, 112−122.

(2) Chong, C.; Mishra, H.; Boukheddaden, K.; Denise, S. p.; Bouchez, G.; Collet, E.; Ameline, J. C.; Naik, A. D.; Garcia, Y.; Varret, F. Electronic and structural aspects of spin transitions observed by optical microscopy. The case of $[Fe(ptz)_6](BF_4)_2$. *J. Phys. Chem. B* **2010**, *114*, 1975-1984.

(3) Garcia, Y.; Wang, J; Zhang, T. Mösbauer spectroscopy, Wiley-VCH **2024**.

(4) Fourati, H.; Ndiaye, M.; Sy, M.; Triki, S.; Chastanet, G.; Pillet, S.; Boukheddaden, K. Light-induced thermal hysteresis and high-spin low-spin domain formation evidenced by optical microscopy in a spin-crossover single crystal. *Phys. Rev. B* **2022**, *105*, 174436.

(5) Boukheddaden, K.; Fourati, H.; Singh, Y.; Chastanet, G. Evidence of photo-thermal effects on the first-order thermo-induced spin transition of $[\{Fe(NCSe)(py)_2\}_2(m\text{-bpypz})]$ spin-crossover material. *Magnetochemistry* **2019**, *5*, 21.